DALTON
FULL PAPER

Theoretical studies of metal complexes of anhydrotetracycline: interaction with Zn^{II} †

Wagner B. De Almeida,*[a,b] Hélio F. Dos Santos,[a] William R. Rocha[a] and Michael C. Zerner[b]

[a] *Laboratório de Química Computacional e Modelagem Molecular, Departamento de Química, ICEx, UFMG, Belo Horizonte, MG, 31270-901, Brazil*
[b] *Quantum Theory Project, University of Florida, Gainesville, Florida, 32611-8435, USA*

A quantum mechanical semiempirical study (AM1) of the interaction of anhydrotetracycline (AHTC) with zinc(II) has been reported. All possible complexation sites were examined and structures of complexes containing two and four water molecules were fully optimized. The solvent effect was included using macroscopic dielectric models for calculating solvation energies in aqueous solution. It was predicted that the four-co-ordinated complexes are favored in solution and the six-co-ordinated complexes are predominant in the gas phase. Comparison with recent experimental investigations, conducted in aqueous solution, is made. The theoretical results agree well with the sparse experimental information that is available on the molecular structure of the Zn^{II}–AHTC complex, allowing predictions to be made on the structures of related complexes not yet determined.

Tetracycline [TC, Fig. 1(*a*)] is the parent compound of a widely used group of antibiotics. The treatment of TC by warm mineral acids leads to the aromatization of the C ring by removal of one water molecule from the atomic positions 5a and 6 [see Fig. 1(*a*)]. The anhydrous derivative, anhydrotetracycline [AHTC, Fig. 1(*b*)] presents low bacteriostatic activity and has been considered responsible for many side effects observed upon ingestion of the drug beyond its limit of validity.[1,2] Despite the aromatization of the C ring, the loss of activity and the toxic effects of AHTC have been discussed as a function of the relative position of the A ring when compared with solid state structures of active compounds.[3]

The free base of tetracycline derivatives plays an important role for the biological activity.[4–6] However, it has been shown that the free forms of these drugs in blood plasma occur at insignificant levels during treatment since complexes of Ca and Mg are predominant in the fraction of the drug not bound to protein.[7] As does the parent compound, AHTC contains several potential binding sites for metal ions. In addition to the phenolate oxygens at C10 and C11, and the carbonyl one at C12 in the BCD ring system, the molecule presents different co-ordination positions on ring A. These are the amide and the dimethylamine groups at C2 and C4 respectively, the enolic function at C3 and the carbonyl group at C1. The interactions of the antibiotic with Zn were shown to be important in the gastrointestinal tract, and it was observed that the metal plays an antagonistic role on the gastrointestinal absorption of the drug.[8]

The complexation of tetracyclines with other essential or non-essential metal ions has been the object of extensive studies.[9] Recently, experimental studies on the free AHTC molecule and respective metal complexes were reported by Beraldo and co-workers for Cu^{II} and Ni^{II},[10] Mg^{II}, Al^{III} and Fe^{III} [11] and Cu^{II} and Zn^{II} [12]. The formation of metal complexes has been addressed and the structure and possible sites for complexation have been suggested based on the analysis of absorption and circular dichroism (CD) spectra in aqueous solution. In the light of these experimental results, we decided to carry out a quantum mechanical study of the AHTC molecule and its metal complexes with the purpose of examining its structural and spectroscopic properties. The free AHTC species have been examined in previous works.[13,14] In this study

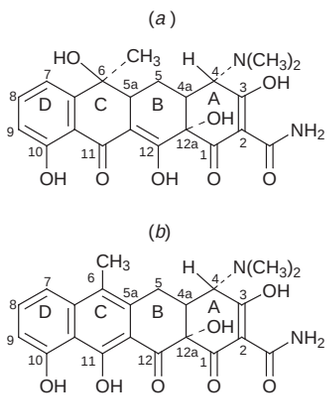

Fig. 1 Numbering scheme for TC (*a*) and AHTC (*b*) molecules. The abbreviations am, m1 and m2, used for dihedral angles definition, refer respectively to the amide (at C2) and dimethylamine (at C4) groups. Definition of the main dihedral angles: ω_1, O12a,C12a,C4a,H4a; ω_2, C4,C4a,C12a,C1; ω_3, C12,C12a,C4a,C5; ω_4, C1,C2,C2am,O2am; ω_5, C3,C4,N4,Cm1; ω_6, C3,C4,N4,Cm2

we report a quantum chemical investigation of the potential energy surface (PES) for the interaction of the AHTC ionized species present at neutral pH (HL^-) with zinc(II). The present work aims to combine the new theoretical results with the available experimental information for a better understanding of the molecular structure of the AHTC–Zn^{II} complex. Such a study can help in understanding the complexation process at a molecular level.

Calculations

The free AHTC molecule was previously studied by us [14] using the AM1 (Austin Model 1) quantum mechanical semiempirical method.[15] The molecular structures of the non-ionized (H_2L) and the ionized forms [H_3L^+, $H_2L^{\pm}$ (zwitterionic form), HL^- and L^{2-}] were calculated. The deprotonated species were obtained from H_3L^+ by subsequent removal of hydrogen atoms. It was shown [14] that there is good agreement between the gas phase calculated and observed crystallographic structures [3] of the fully protonated species H_3L^+. From the study of the species distribution as function of the pH for AHTC,[10] it was found that the following species are present at more than 90% for pH values 1 (H_3L^+), 4.6 ($H_2L^{\pm}$), 7 (HL^-) and greater than 10 (L^{2-}). The present work aims to investigate the interaction of the

† *Non-SI unit employed*: cal = 4.184 J.

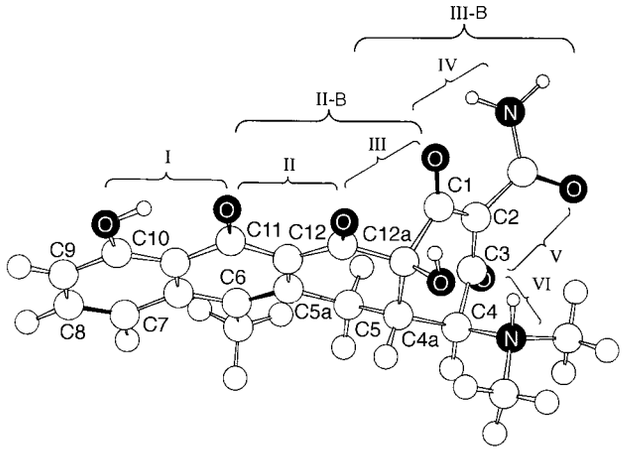

Fig. 2 The AM1 fully optimized geometry of the HL^-(O11) structure, showing the possible metal complexation sites: I (O10–O11), II (O11–O12), III (O12–O1), IV (O1–Nam), V (O3–Oam), VI (O3–N4), II-B (O11–O12–O1) and III-B (O12–O1–Oam)

AHTC with Zn^{II} at neutral pH,[12] that is the complexation of the HL^- species with zinc(II) ions. Fig. 2 shows the possible metal complexation sites, designated I(O10–O11), II(O11–O12), III(O12–O1), IV(O1–Nam), V(O3–Oam), VI(O3–N4), and tridentate II-B(O11–O12–O1), III-B(O12–O1–Oam). In order to sample the full conformational space, several distinct initial trial structures were used in a comprehensive investigation of stationary points present on the potential energy surface for the Zn^{II}–AHTC complex. All fully optimized stationary points were further characterized as true minimum energy structures with the aid of harmonic frequency analysis. The AM1 parameters for the zinc atom are given in ref. 16. A complete conformational analysis for the free ligand has been carried out previously[14] and the possible geometrical positions for the Zn^{II} are indicated in Fig. 2. Exhaustive full geometry optimizations have been made using distinct initial guesses varying the spatial orientation of the metal ion. Therefore, we can assure that a complete conformational analysis for the Zn^{II}–AHTC complexes has been accomplished.

Processes (1)–(4) were assumed to take place with the formation of tetrahedral and octahedral complexes. These reactions involve hydrated species and so the thermodynamic cycles involving solutions have to be considered (Schemes 1 and 2).

$$[Zn(H_2O)_6]^{2+} + HL^- \longrightarrow [Zn(HL)(H_2O)_2]^+ + 4H_2O \quad \text{(tetrahedral)} \quad (1)$$

$$[Zn(H_2O)_6]^{2+} + HL^- \longrightarrow [Zn(HL)(H_2O)_4]^+ + 2H_2O \quad \text{(octahedral)} \quad (2)$$

$$2[Zn(H_2O)_6]^{2+} + HL^- \longrightarrow [Zn_2L(H_2O)_4]^{2+} + H_3O^+ + 7H_2O \quad \text{(tetrahedral)} \quad (3)$$

$$2[Zn(H_2O)_6]^{2+} + HL^- \longrightarrow [Zn_2L(H_2O)_8]^{2+} + H_3O^+ + 3H_2O \quad \text{(octahedral)} \quad (4)$$

The solvation energy is evaluated as the difference between the energy contributions from products and reagents, equations (5)–(7). We can estimate the energy of solution for the products

$$\Delta E(\text{aq}) = \Delta E(\text{gas}) + [\Delta E_{\text{P}}(\text{sol}) - \Delta E_{\text{R}}(\text{sol})] \quad (5)$$

$$\Delta E(\text{gas}) = E\{[Zn(HL)(H_2O)_n]^+\} + (6 - n)E(H_2O) - (E\{[Zn(H_2O)_6]^{2+}\} + E[HL^-(O11)]) \quad \text{(Scheme 1)} \quad (6)$$

$$\Delta E(\text{gas}) = E\{[Zn_2L(H_2O)_n]^+\} + (11 - n)E(H_2O) + E(H_3O^+) - (2E\{[Zn(H_2O)_6]^{2+}\} + E[HL^-(O11)]) \quad \text{(Scheme 2)} \quad (7)$$

and reagents from the Born equation for ions, and from the $\Delta E_{\text{vap}} = +9.5$ kcal mol^{-1} for water, as in expression (8) where

$$\Delta E_1^{\text{sol}} = -\{166[1 - (1/\varepsilon)]q^2/a_0\} - 9.5n \quad (8)$$

$\varepsilon = 78.5$ for H_2O, q = charge of the species (free ligand, $[Zn(H_2O)_6]^{2+}$ pr Zn–AHTC complexes), n = number of moles of water, 9.5 = heat of vaporization of water, a_0 = cavity radius = $0.732(M/\rho)^{\frac{1}{3}}$, M = molecular mass and ρ = density assumed to be 1 g cm^{-3}. The Born term is the first term in a multipole expansion of the electrostatic potential, and dominates in the case of charged species. The second contribution, the Onsager term, involves the stabilization of a dipole in a medium with relative permittivity ε, which is given by[17] equation (9)

$$\Delta E_2^{\text{sol}} \approx -166\frac{(2\varepsilon - 2)}{(2\varepsilon + 1)}(P_e^2/a_0^3) \quad (9)$$

where P_e = dipole moment. For high dielectrics, such as water, the COSMO (conductor-like screening model)[18] is attractive, as it solves directly Poisson's equation for arbitrary shape. We applied this model using the gas phase AM1 fully optimized geometries to obtain ΔE^{COSMO}.

The total Gibbs free energy difference, between products and reagents in the gas phase, is evaluated according to expression (10), where ΔE^{zero} is the zero point energy contribution. The free energy of solvation is given by equations (11)–(13).

$$\Delta G_{\text{gas}}^{\text{total}} = \Delta G_{\text{trans}} + \Delta G_{\text{vib}} + \Delta G_{\text{rot}} + \Delta E(\text{gas}) + \Delta E^{\text{zero}}; \quad G = H - TS \quad (10)$$

$$\Delta G_{1\,(\text{aq})}^{\text{total}} = \Delta G_{\text{gas}}^{\text{total}} + \Delta E_1^{\text{sol}} \quad (11)$$

$$\Delta G_{2\,(\text{aq})}^{\text{total}} = \Delta G_1^{\text{total}}(\text{aq}) + \Delta E_2^{\text{sol}} \quad (12)$$

$$\Delta G_{\text{cosmo}}^{\text{total}} = \Delta G_{\text{gas}}^{\text{total}} + \Delta E^{\text{COSMO}} \quad (13)$$

Results and Discussion

Some *ab initio* results for model complexes are quoted in Table 1 in order to assess the validity of using the AM1 semiempirical method for the calculation of geometries and stabilization energies for the Zn^{II}–AHTC complexes. Our *ab initio* results

$$\begin{array}{ccc} [Zn(H_2O)_6]^{2+}(\text{gas}) + HL^-(O11)(\text{gas}) & \xrightarrow{\Delta E(\text{gas})} & [Zn(HL)(H_2O)_n]^+(\text{gas}) + (6-n)H_2O(\text{gas}) \\ -\Delta E_{\text{R}}(\text{sol}) \uparrow & & \downarrow \Delta E_{\text{P}}(\text{sol}) \\ [Zn(H_2O)_6]^{2+}(\text{aq}) + HL^-(O11)(\text{aq}) & \xrightarrow{\Delta E(\text{aq})} & [Zn(HL)(H_2O)_n]^+(\text{aq}) + (6-n)H_2O(\text{aq}) \end{array}$$

Scheme 1

$$\begin{array}{ccc} 2[Zn(H_2O)_6]^{2+}(\text{gas}) + HL^-(O11)(\text{gas}) & \xrightarrow{\Delta E(\text{gas})} & [Zn_2L(H_2O)_n]^{2+}(\text{gas}) + H_3O^+ + (11-n)H_2O(\text{gas}) \\ -\Delta E_{\text{R}}(\text{sol}) \uparrow & & \downarrow \Delta E_{\text{P}}(\text{sol}) \\ 2[Zn(H_2O)_6]^{2+}(\text{aq}) + HL^-(O11)(\text{aq}) & \xrightarrow{\Delta E(\text{aq})} & [Zn_2L(H_2O)_n]^{2+}(\text{aq}) + H_3O^+ + (11-n)H_2O(\text{aq}) \end{array}$$

Scheme 2

Table 1 Interaction energies (ΔE) for $Zn^{2+} + nL^{k-} \longrightarrow [ZnL]^{(2-k)+}$ and metal–ligand distances d(Zn–X) for some zinc(II) model complexes

	ΔE/kcal mol^{-1}				d(Zn–X)[a]/Å		
Complex	AM1	HF/SCF(ECP)[b]	MP2[c]	MP2[d]	AM1[d]	HF/SCF(ECP)[b]	MP2[d]
$[Zn(H_2O)]^{2+}$	−112.4	−88.7	−95.6		2.00	1.90	
$[Zn(H_2O)_2]^{2+}$	−183.1	−159.8		−181.32	2.11	2.0	1.90
$[Zn(H_2O)_4]^{2+}$	−257.7	−260.0		−296.95	2.10	2.0	2.02
$[Zn(H_2O)_6]^{2+}$	−298.4	−303.6		−367.23	2.20	2.1	2.12
$[Zn(HCO_2)]^{+}$	−435.2	−380.0	−404.0		2.10	1.98	
$[Zn(NHMe_2)]^{2+}$	−189.4	−131.7	−151.9		2.01	1.98	

[a] X = O or N atom; HF/SCF(ECP) geometries were not fully optimized. [b] See ref. 19. The C,N and O core, and the first two occupied shells of Zn^{II}, are represented by the atomic compact effective potential derived by Hay and Wadt.[20] The hydrogen basis set and valence basis sets of the heavy atoms consist of four gaussians, contracted (3,1). The heavy atoms are supplemented with a set of two diffuse uncontracted 3d orbitals. See also refs. 21 and 22. [c] See ref. 21. [d] The present work using the 6-31G(d) and STO-3G basis sets respectively for ligand heavy atoms and hydrogen atoms. Effective core potential and valence double zeta basis set used for the zinc atom.

Table 2 The AM1 energies[a] (kcal mol^{-1}) for the $[Zn(HL)(H_2O)_2]^{+}$ and $[Zn(HL)(H_2O)]^{+}$ tetrahedral complexes

	Complexation sites									
	I[b]	II	III	IV	IV-A[c]	V[d],VI[e]	II-A[f,g]	II-B[f,h]	III-A[g,i]	III-B[i]
Gas phase calculation										
ΔG_{gas}^{total}	−189.18	−202.35	−206.41	−190.27	−197.01		−209.11	−209.49	−207.21	−207.91
$\Delta(\Delta G_{gas}^{total})$	20.31	7.14	3.08	19.22	12.48		0.38	0.0	2.28	1.58
Solvation enery calculation										
$\Delta G_1{}^{total}_{(aq)}$	−64.45	−77.62	−81.68	−65.54	−72.28		−84.38	−94.54	−82.98	−92.96
$\Delta[\Delta G_1{}^{total}_{(aq)}]$	30.09	16.92	12.86	29.0	22.26		10.16	0.0	11.56	1.58
$\Delta G_2{}^{total}_{(aq)}$	−61.20	−71.18	−77.00	−65.03			−79.81	−90.16	−78.79	−90.62
$\Delta[\Delta G_2{}^{total}_{(aq)}]$	29.42	19.44	13.62	25.59			10.81	0.46	11.83	0.0
ΔG_{cosmo}^{total}	−27.03	−34.72	−26.49	−33.72	−31.36		−16.39	−35.30	−14.85	−34.94
$\Delta(\Delta G_{cosmo}^{total})$	8.27	0.58	8.81	1.58	3.94		18.91	0.0	20.45	0.36

[a] Calculated using equations (5)–(13), given in the Calculations section. [b] In this structure the hydrogen atom attached to the O10 group moves to the O12 group, similar to a tautomerism. [c] The Zn^{II} is bonded to the O1 and Oam oxygen atoms. [d] The HL^{-} ligand assumes a conformation quite distinct from the free AHTC in this complex and which is not related to the other structures. [e] There is no stable structure for the complexation of Zn^{II} at this site for the HL^{-} ligand. [f] These structures involve three oxygen atoms, O11–O12–O1, tridentate mode, which is a combination of sites II and III. [g] Co-ordination number of Zn^{II} is 5; two water molecules are bonded to the zinc atom. [h] Co-ordination number of Zn^{II} is 4; only one water molecule is bonded to the zinc atom. [i] This structure involves three oxygen atoms, O12–O1–Oam, tridentate mode, which is a combination of sites III and IV.

were obtained from symmetry unconstrained geometry optimizations at the second-order Møller-Plesset perturbation theory (MP2) level. The effective core potential (ECP) and valence double zeta basis set of Hay and Wadt[20] for Zn atoms, which include 4d, 5s and 6p orbitals for the zinc atom, were used. The spilt-valence 6-31G(d) basis set,[23] which includes a set of five d polarization functions was used for the oxygen atom. Since the hydrogen atoms do not belong to the 'reactive system' they were treated as 'spectator' atoms and a minimum basis set STO-3G[23] was used for them.

The chosen model ligands contain the groups in the free AHTC molecule that are potential binding sites for metals. From Table 1 it can be seen that the AM1 approach consistently produces good metal–ligand distance values. Comparing the stabilization energies it can further be seen that the AM1 method appears to overestimate the interaction energies for the one- and two-co-ordinated complexes and underestimate the energies of the respective four- and six-co-ordinated complexes relative to the *ab initio* results. However the energy trends are quite satisfactorily predicted and the much more efficient AM1 model is thus expected to yield trustable relative energy values for the distinct conformations resulting from the complexation of Zn^{II} at different sites of the AHTC ligand.

The ability of the AM1 method for predicting structural parameters for large molecules containing atoms of the second row of the Periodic Table has been verified in some cases where crystal structures are available.[24] We have also been able to reproduce successfully the crystallographic structure of the free ligand.[14] With the aim of examining the semiempirical structural parameters for metal complexes we have carried out a full geometry optimization of the global minimum on the PES for the Al^{III}–AHTC metal complex[25] at the *ab initio* Hartree–Fock level of theory. We found that the Hartree–Fock and AM1 geometries are essentially the same. Therefore, we have reasons to trust the AM1 calculated geometries for the Zn^{II}–AHTC complexes.

Tables 2 and 3 report the AM1 interaction energies and Gibbs free energy of solvation for the possible tetrahedral structures resulting from the interaction of Zn^{II} with the AHTC molecule at neutral pH. The energies given were evaluated using equations (5)–(13). The complexation at site VI only takes place when the proton attached to the N4 atom is removed, generating the so-called L^{2-} species. In the present study no stable structures were found for the complexation of Zn^{II} at this site when monometallic complexes were considered. It appears that this complexation site will only play a role for the Zn_2–AHTC complex. In addition, the complexation at site V leads to a quite distorted structure of the HL^{-} ligand, which has no resemblance with the free form of AHTC predicted to exist at neutral pH. Therefore, the complexation site V, which is also energetically higher, will not be further considered.

We have investigated the four- and six-co-ordinated complexes in the gas phase and including solvent effects using macroscopic dielectric models for calculating solvation energies in aqueous solution, employing the equations given in the Calculations section. We found that the six-co-ordinated complexes are predicted to be favored in the gas phase. However, according to our solvation energy calculations, the four-co-ordinate species should be dominant in aqueous solution. Therefore we concentrate our discussion on the tetrahedral complexes and the results and figures concerning the octahedral species are available directly from the authors.

Table 3 The AM1 energies* (kcal mol^{-1}) for the $[Zn_2L(H_2O)_4]^{2+}$ and $[Zn_2L(H_2O)_3]^{2+}$ bimetallic complexes

	Complexation site				
	I/VI	II/VI	III/VI	IV/VI	II-B/VI
Gas phase calculation					
ΔG_{gas}^{total}	−216.66	−219.81	−201.67	−174.71	−205.05
$\Delta(\Delta G_{gas}^{total})$	3.15	0.0	18.14	45.07	14.76
Solvation energy calculation					
$\Delta G_{1\ (aq)}^{total}$	−120.79	−123.94	−105.80	−78.87	−119.64
$\Delta[\Delta G_{1\ (aq)}^{total}]$	3.15	0.0	18.14	45.07	4.30
$\Delta G_{2\ (aq)}^{total}$	−116.81	−121.95	−137.63	−103.68	−131.91
$\Delta[\Delta G_{2\ (aq)}^{total}]$	20.82	15.68	0.0	33.95	5.72
ΔG_{cosmo}^{total}	−56.22	−61.43	−46.04	−55.70	−58.80
$\Delta(\Delta G_{cosmo}^{total})$	5.21	0.0	15.39	5.73	2.63

* Calculated using equations (5)–(13), given in the Calculations section.

According to our gas phase total energy difference [ΔE(gas)] results the tridentate five-co-ordinated species (II-A) is dominant when two water molecules are co-ordinated to the Zn^{II}. The Gibbs free energy results show that the entropy contribution plays an important role for complexes with a single zinc atom (Table 2). When the zero point energy (ΔE^{zero}) and Gibbs free energy (ΔG) are combined with the total energy difference between different conformers [ΔE(gas)], producing ΔG_{gas}^{total}, the conformational preferences change dramatically from the results obtained using only gas phase total energy differences. The structures II-B (tridentate four-co-ordinated with only one water molecule bonded to the Zn^{II}) and II-A (five-co-ordinated) are now predicted to be dominant with a preference for II-B.

We caution here, however, that these calculations are likely no better in producing relative energies than ±2 kcal mol^{-1} which has a large effect on relative abundance. What is really suggested here is that II-A and II-B are likely the dominant structures. This proviso should be considered in all subsequent discussion of structures that are close in energy. Therefore, these are the most probable species to be found in the gas phase. Adding the solvation energy contribution to the total Gibbs free energy variation leads to a significant change (see Table 2). The Born model and the COSMO approach predict the II-B tridentate structure as the predominant one followed by the other tridentate four-co-ordinate III-B complex. The charge plus dipole model for solvation energy calculations predicts an almost 50% equilibrium between the two tridentate structures II-B and III-B.

For the metal complex containing two zinc atoms the interactions of Zn^{II} at sites II and VI are predicted to be the most favored on energy grounds (Table 3). For the $[Zn_2L(H_2O)_4]^{2+}$ complex (Table 3) the II/VI structure is always dominant no matter whether the entropy contribution is included or not. The gas phase and solvation energy results for the $[Zn_2L(H_2O)_4]^{2+}$ complex both lead to structure II/VI as predominant, but the charge plus dipole model predicts III/VI as the only one to be observed experimentally. Certainly, the much bigger permanent dipole moment of structure III/VI as compared with II/VI is affecting the energy balance favoring the complex II/VI.

Figs. 3 and 4 show the most relevant structures for the complexes having a single zinc atom co-ordinated to the AHTC ligand. The corresponding figures for the six-co-ordinated complexes are available directly from the authors. The main geometrical parameters are also given. From these figures it can be seen that the relative position of the amide group changes significantly depending on which complexation site is activated. In the free HL^- species the amide oxygen atom is *trans* with respect to the carbonyl group at position C1, with a dihedral angle of 140° (AM1 value). An X-ray value of 183° has been reported for the H_3L^+ species.[3] The respective value for the free L^{2-} species is 146° (AM1 value from ref. 14). For some zinc(II)

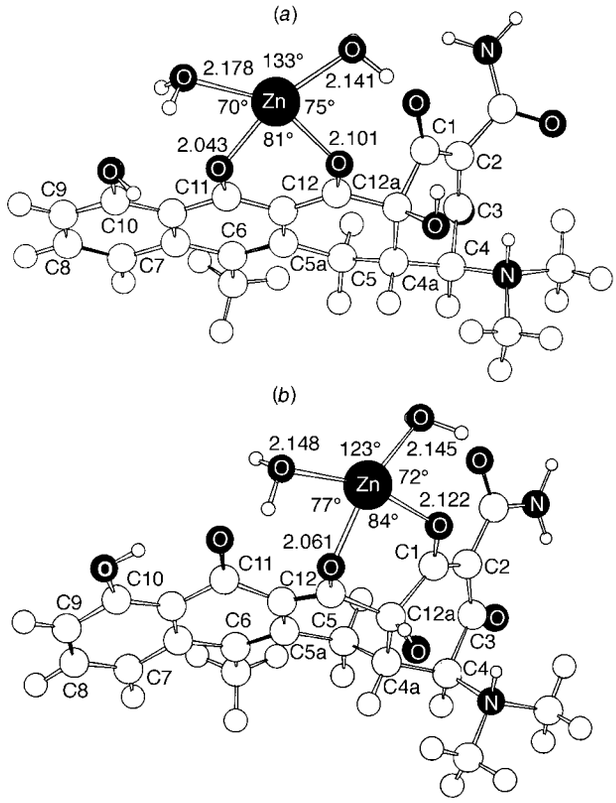

Fig. 3 The AM1 optimized structures (bond lengths in Å) of the $[Zn(HL)(H_2O)_2]^+$ complex: (*a*) complexation site II and (*b*) complexation site III

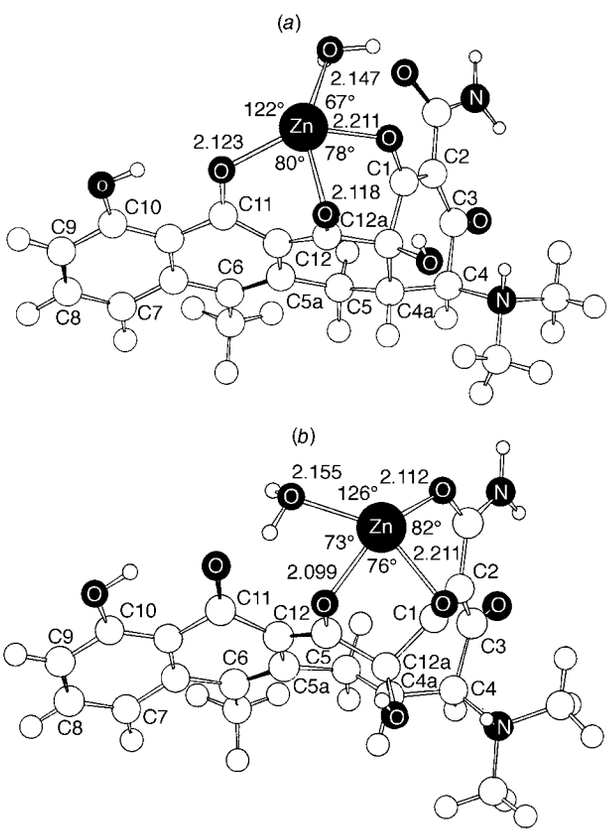

Fig. 4 The AM1 optimized structures (bond lengths in Å) of the tridentate complex $[Zn(HL)(H_2O)]^+$: (*a*) II-B and (*b*) III-B

complexes the *cis* orientation of the amide oxygen atom is preferred, for example structures III and II-A of $[Zn(HL)(H_2O)_4]^+$. The AHTC ligand distorts significantly upon complexation with Zn^{II} at certain sties. The basic reason for this behavior is

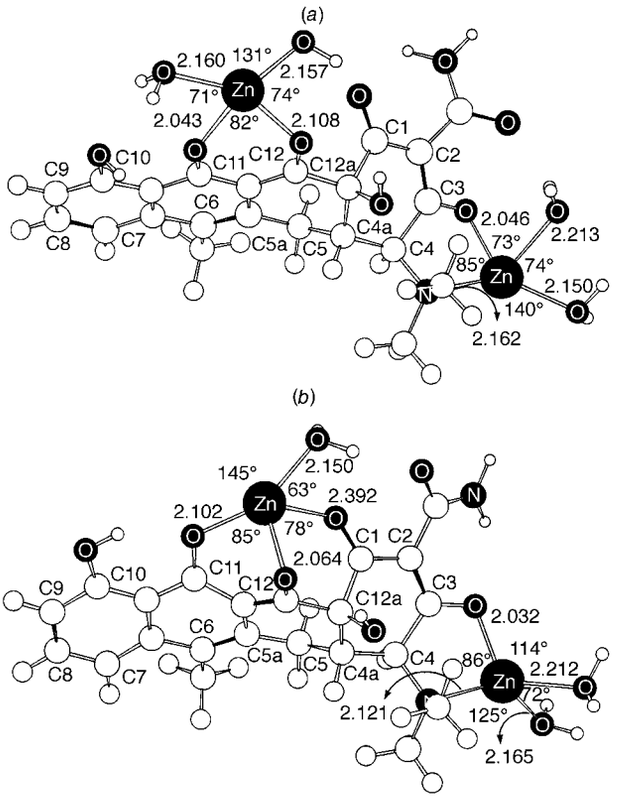

Fig. 5 The AM1 optimized structures (bond lengths in Å) of the complex $[Zn_2L(H_2O)_4]^{2+}$: (*a*) II/VI and (*b*) II-B/VI

the formation of intramolecular hydrogen bonds, as can be easily visualized by looking at Figs. 3–5. The H_2N–C=O group rotates in order to minimize the interaction energy which leads to the formation of hydrogen bonds with the water molecules co-ordinated to the zinc atom, which is important only when the metal co-ordination occurs at the sites III and II-A (or II-B) [see Figs. 3(*b*), 4(*a*), 4(*b*) and 5(*b*)].

According to the gas phase calculations for the free AHTC (HL^- species), the PES for the rotation of the amide group around the C2–C2am bond exhibits only two identical *trans* minima connected *via* a transition state (TS) structure 8.5 kcal mol^{-1} above the minima. There is a second *cis* minimum in this region of the PES, which is 6.1 kcal mol^{-1} energetically higher than the first. However, when the rotation around the C2–C2am bond takes place no energy barrier is found; that is, the second local *cis* minimum converts spontaneously into the first one (*trans*). This suggests that it is not possible to observe the structure where the orientation of the amide oxygen atom is *cis* to O1 for the free AHTC molecule. In their article on the crystal and molecular structures of anhydrotetracycline hydrobromide monohydrate (henceforth AHTC·HBr) and 6-demethyl-7-chlorotetracycline hydrochloride trihydrate (henceforth 6-DM-7-CITC·HCl), Palenik *et al.*[3] found that the anhydrotetracyclinium and 6-demethyl-7-chlorotetracyclinium cations showed a distinct orientation of the amide oxygen in relation to O1. The amide oxygen orientation is *trans* to O1 in $AHTC{\cdot}H^+$ and *cis* for the 6-DM-7-$CITC{\cdot}H^+$, as in the parent compound tetracycline. They expected that the barrier for rotation of the amide group might be high. Our explanation for this fact is that there is a free conformational interconversion in this case. However, in the Zn–AHTC complexes this second isomer is frequently present. As mentioned before, the approach of the Zn atom causes the *cis* relative position of the amide group to be favored over the *trans* isomer, for certain complexation sites, because of intramolecular hydrogen bonds.

Another important issue of the present work concerns the deprotonation sites O10 and O11 (see Fig. 1). Based on experimental information it was proposed that the second deprotonation of the H_3L^+ species occurs at the phenolic proton at O10 with the formation of the HL^- species.[10] The first deprotonation site was assigned to the enolic proton at O3.[10] According to our calculations both O10 and O11 sites are probable candidates for deprotonation. The gas phase energy difference between the O10 and O11 free HL^- deprotonated species is 4 kcal mol^{-1}, favoring the O11 site. For all minimum energy structures located on the PES for the Zn–AHTC complexes the deprotonation at O11 is favored by more than *ca.* 20 kcal mol^{-1} in the gas phase. We have also studied the O10 and O11 free HL^- relative population in solution using the solvation models described in the Calculations section.[26] Inclusion of the solvation energy, calculated for a frozen gas phase equilibrium geometry, favors the O11 deprotonation site, leaving no doubt that the main AHTC free species present at neutral pH is deprotonated at the O11 position.

Finally, we discuss the molecular structure of the preferred complexation sites for the interaction between the Zn^{II} and the AHTC molecule. From Figs. 3–5 it can be seen that there is significant deviation from perfect tetrahedral structures. The reason for this is the formation of hydrogen bonds, which stabilize the complex formation. Table 4 gives the main dihedral angles related to the A and B rings for the Zn^{II}–AHTC complexes and the respective values for the free AHTC species. It can be seen from this table that the position of the dimethylamine group is practically unchanged in the series of structures of metal–AHTC complexes calculated. Exception is made for complexes involving two zinc atoms, since one of the atoms is bonded to the dimethylamine group.

According to our calculations the four-co-ordinate tridentate structure, II-B is favored for the Zn–AHTC complex at neutral pH (followed by the III-B species) while the structure II/VI is preferred for the respective complexes with two zinc atoms, *i.e.* $[Zn_2L(H_2O)_4]^{2+}$. Therefore there are three plausible co-ordination modes for the Zn^{II} involving different numbers of co-ordinated water molecules, *i.e.* tridentate four-co-ordinate II-B (predominant) and III-B species, and four-co-ordinate dizinc complexes, with the zinc atoms bound at sites II and VI. These are the possible Zn^{II}–AHTC complex candidates to be observed in neutral pH. For the complex of a single zinc atom there is a competition between the two tridentate $[Zn(HL)(H_2O)]^+$ structures II-B and III-B with a predominance of II-B. Considering the complexes with two zinc atoms structure II/VI is predominant in aqueous solution.

These results are in agreement with the complexation sites suggested experimentally, based on electronic spectra studies in aqueous solution at neutral pH.[12] In the experimental study, Matos and Beraldo[12] proposed that a juxtaposition of O1, O11 and O12 would allow the AHTC ligand to co-ordinate in a tridentate fashion. They assumed that the geometry of the complex is probably tetrahedral with a water molecule occupying the fourth co-ordination site. Our theoretical results show that the four-co-ordinate complex is indeed energetically favored. However, the tridentate mode of co-ordination of the AHTC ligand is not operative for the complexation with two zinc atoms. The presence of the second zinc atom favors substantially the O11–O12 complexation site.

The theoretical calculations and the experimental studies in aqueous solution definitively agree that the O11–O12–O1 (tridentate II-III mode) complexation site is the preferred one for the complexation of a single zinc atom with AHTC. In addition the second complex involving complexation of zinc to the nitrogen of the methylamine group may exist, and the excess of Zn^{II} would lead to complexation at sites II and VI (see Fig. 3).

Conclusion

The AM1 calculations were performed in order to elucidate the molecular structure of the complexes formed between Zn^{II} and AHTC. All possible metal complexation sites were investigated

Table 4 The AM1 dihedral angles (A and B rings) for the mono- and bi-metallic tetrahedral Zn–AHTC complexes. The corresponding values for the free ionized forms of AHTC are given for comparison

	Co-ordination sites $[Zn(HL)(H_2O)_2]^+$ and $[Zn(HL)(H_2O)]^+$									
	I[a]	II	III	IV	IV-A[b]	II-A[c,d]	II-B[c,e]	III-A[d,f]	III-B[d,f]	HL^{-}[g]
O12a–C12a–C4a–H4a	42	44	44	44	47	48	48	24	25	48
C4–C4a–C12a–C1	40	41	41	43	46	48	48	24	24	42
C12–C12a–C4a–C5	45	46	43	41	44	44	43	20	20	52
C1–C2–C2am–O2am	141	138	−13	126	0	−15	−15	−13	−13	140
C3–C4–N4–Cm1	−176	−175	180	180	179	178	178	−161	−160	−177
C3–C4–N4–Cm2	−52	−51	−56	−56	−58	−59	−59	−38	−37	−52

	Co-ordination sites $[Zn_2L(H_2O)_4]^{2+}$ and $[Zn_2L(H_2O)_3]^{2+}$					
	I/VI^{+}[a]	II/VI	III/VI	IV/VI	II-B/VI[h]	L^{2-}[g]
O12a–C12a–C4a–H4a	51	49	50	46	50	47
C4–C4a–C12a–C1	50	47	48	44	50	43
C12–C12a–C4a–C5	50	48	43	40	42	50
C1–C2–C2am–O2am	137	134	24	138	16	146
C3–C4–N4–Cm1	−154	−154	−156	−153	−155	−61
C3–C4–N4–Cm2	78	79	77	80	77	170

[a] In this structure the hydrogen atom attached to the O10 group moves to the O12 group, similar to a tautomerism. [b] The Zn^{II} is bonded to the O1 and Oam oxygen atoms. [c] This structure involves three oxygen atoms, O11–O12–O1, tridentate mode, which is a combination of sites II and III. [d] Co-ordination number of Zn^{II} is 5; two water molecules are bonded to the zinc atom. [e] Co-ordination number of Zn^{II} is 4; only one water molecule is bonded to the zinc atom. [f] This structure involves three oxygen atoms, O12–O1–Oam, tridentate mode, which is a combination of sites III and IV. [g] AM1 data from ref. 14. [h] In this structure the first zinc atom is bonded to the O11–O12–O1 oxygen atoms, tridentate mode. Both zinc atoms have co-ordination number four.

between one and two zinc(II) ions and AHTC. On the basis of these calculated interaction energies the six-co-ordinated structures are predicted to be the preferred ones for the Zn–AHTC and Zn_2–AHTC complexes in the gas phase. In neutral water solution, the four-co-ordinate complexes are preferred in relation to the six-co-ordinated Zn–AHTC species. The tridentate mode of complexation of the AHTC ligand was favored in our calculations. The tridentate structure II-B is predicted to be favored for the four-co-ordinate complex, followed by the other tridentate III-B structure. For the Zn_2–AHTC four-co-ordinate complex, the combined complexation sites II and VI are predicted to be the favored mode both in the gas phase and water solution. Contrary to the experimental proposal, a tetrahedral complex for dizinc species, with the AHTC acting as a tridentate ligand, is not supported by our calculations.

Another important issue of the present theoretical study concerns the second deprotonation site of the free AHTC species. Based on experimental evidence the HL^{-} species was predicted to be deprotonated at O3 (first deprotonation site) and O10 (second deprotonation site) in aqueous solution at neutral pH.[10] Our calculations suggest that the second deprotonation site is O11. We estimate that the O11 site is 4 kcal mol^{-1} energetically favored in the free AHTC species and more than 20 kcal mol^{-1} more stable than the O10 site for the Zn–AHTC complex (gas phase results). The same behavior was observed when solvation effects were included in the relative energy calculations.

Acknowledgements

W. B. De Almeida would like to thank the Fundação Co-ordenação de Aperfeiçoamento de Pessoal de Nível Superior (CAPES) for a research grant and also the Fundação de Amparo a Pesquisa do Estado de Minas Gerais (FAPEMIG) and Programa de Apoio ao Desenvolvimento Científico e Tecnológico (PADCT-Proc. No. 62.0241/95.0) for partially supporting this project. H. F. Dos Santos and W. R. Rocha thank the Conselho Nacional de Desenvolvimento Científico e Tecnológico (CNPq) for their research grants. This work was supported in part through a grant from the office of Naval Research.

References

1 A. Alvarez Fernandes, V. T. Torre Noceda and E. S. Sanchez Cabrera, *J. Pharm. Sci.*, 1969, **58**, 443.
2 T. Hasan, M. Allen and B. S. Cooperman, *J. Org. Chem.*, 1985, **50**, 1755.
3 G. J. Palenik, M. Mathew and R. Restivo, *J. Am. Chem. Soc.*, 1978, **100**, 4458.
4 A. I. Laskin and J. A. Last, *Antibiot. Chemother.*, 1971, **17**, 1.
5 F. Peradejordi, A. N. Martin and A. Cammarat, *J. Pharm. Sci.*, 1971, **60**, 576.
6 G. H. Miller, H. L. Smith, W. L. Rock and S. Hedberg, *J. Pharm. Sci.*, 1977, **66**, 88.
7 L. Lambs, M. Brion and G. Berthon, *Inorg. Chim. Acta*, 1985, **106**, 151 and refs. therein.
8 M. Brion, L. Lambs and G. Berthon, *Inorg. Chim. Acta*, 1986, **123**, 61.
9 L. Lambs, B. Decock-Le Révérend, H. Kozlowski and G. Berthon, *Inorg. Chem.*, 1988, **27**, 3001.
10 J. M. Siqueira, S. Carvalho, E. B. Paniago, L. Tosi and H. Beraldo, *J. Pharm. Sci.*, 1994, **83**, 291.
11 F. C. Machado, C. Demicheli, A. Garnier-Suillerot and H. Beraldo, *J. Inorg. Biochem.*, 1995, **60**, 163.
12 S. V. De Mello Matos and H. Beraldo, *J. Braz. Chem. Soc.*, 1995, **6**, 405.
13 W. B. De Almeida, L. R. A. Costa, H. F. Dos Santos and M. C. Zerner, *J. Chem. Soc., Perkin Trans. 2*, 1997, **7**, 1335.
14 H. F. Dos Santos, W. B. De Almeida and M. C. Zerner, *J. Pharm. Sci.*, 1998, **87**, 190.
15 M. J. S. Dewar, E. G. Zoebisch, E. F. Healy and J. J. P. Stewart, *J. Am. Chem. Soc.*, 1985, **107**, 3902.
16 M. J. S. Dewar and K. M. Mertz, *Organometallics*, 1989, **7**, 522.
17 A. Warshel, *Acc. Chem. Res.*, 1981, **14**, 284 and refs. therein.
18 A. Klamt and G. Schuurmann, *J. Chem. Soc., Perkin Trans. 2*, 1993, 799.
19 N. Gresh, *J. Comput. Chem.*, 1995, **16**, 856.
20 P. J. Hay and W. R. Wadt, *J. Chem. Phys.*, 1985, **82**, 270.
21 D. R. Garmer and N. Gresh, *J. Am. Chem. Soc.*, 1994, **116**, 3556.
22 N. Gresh, W. J. Stevens and M. Krauss, *J. Comput. Chem.*, 1995, **16**, 843.
23 W. J. Hehre, R. Ditchfield and J. A. Pople, *J. Chem. Phys.*, 1972, **56**, 2257.
24 H. F. Dos Santos, J. Taylor-Gomer, B. L. Booth and W. B. De Almeida, *Vib. Spectrosc.*, 1995, **10**, 13.
25 W. B. De Almeida, H. F. Dos Santos and M. C. Zerner, *J. Pharm. Sci.*, 1998, in the press.
26 W. B. De Almeida and H. F. Dos Santos, unpublished work.

Received 4*th March* 1998; *Paper* 8/01775A